

P.V. KOSHLIAKOV<sup>1</sup>  
S.R. GORELIK<sup>1,2,✉</sup>  
E.N. CHESNOKOV<sup>1,2</sup>  
A.V. VOROBIEV<sup>1,2</sup>  
A.K. PETROV<sup>1</sup>

# Infrared multiphoton dissociation of vinyltrifluorosilane

<sup>1</sup> Institute of Chemical Kinetics and Combustion SB RAS, Institutskaya, 3, Novosibirsk, 630090, Russia  
<sup>2</sup> Novosibirsk State University, Pirogova, 2, Novosibirsk, 630090, Russia

Received: 27 February 2006/Revised version: 20 April 2006  
© Springer-Verlag 2006

**ABSTRACT** Infrared multiphoton absorption and dissociation of vinyltrifluorosilane molecules under the action of pulsed TEA CO<sub>2</sub>-laser were experimentally studied. The composition of the end dissociation products has been analyzed. Using quantum chemical calculations, we have identified the dissociation pathways that lead to the observed end products. Transition state geometries, enthalpies and activation energies for the dissociation pathways have been calculated. The dissociation channel ratio was determined under used experimental conditions. The silicon isotope selective infrared multiphoton dissociation has been performed at different wavelengths of the CO<sub>2</sub>-laser radiation.

PACS 82.50Bc; 82.30Lp; 31.15.Ew

## 1 Introduction

In the past few years the interest in isotopically pure silicon materials has been growing in the world. It arises from prospects of application of these materials for semiconductor technology. For example, it was shown that the thermal conductivity and the electric conductivity in <sup>28</sup>Si isotopically pure monocrystals are much higher compared to those with natural isotope composition [1, 2]. This fact might be required, in particular for creating more powerful computer processors even today.

Silicon has three stable isotopes with the natural composition: 92.22% (<sup>28</sup>Si) : 4.69% (<sup>29</sup>Si) : 3.09% (<sup>30</sup>Si) [10]. Separation of Si isotopes by means of infrared laser radiation had been studied in [3–9]. In the earliest demonstrations the isotope-selective infrared multiphoton dissociation (IR MPD) of SiF<sub>4</sub> [3] and the isotope-selective reaction of bromination of vibrationally excited silane [4] were studied. However, the most impressive results have been reached in experiments on IR MPD of the species Si<sub>2</sub>F<sub>6</sub> [5–9]. Kamioka et al. [5, 6] reported the IR MPD of Si<sub>2</sub>F<sub>6</sub> molecules induced by CO<sub>2</sub>-laser radiation with high dissociation efficiency and high isotope selectivity. High dissociation yield had been reached with mild radiation fluences lower than 1 J/cm<sup>2</sup>. The maximum isotope content of <sup>30</sup>Si in dissociation products was

nearly 50%, and for <sup>29</sup>Si it was about 12%. It was demonstrated in these works that the isotope-selective IR MPD of the Si<sub>2</sub>F<sub>6</sub> molecules can be the basis for the technological process of silicon-isotope separation with productivity of several grams per hour of the dissociation products enriched to 33% of <sup>30</sup>Si.

Despite such impressive results, it is not evident that Si<sub>2</sub>F<sub>6</sub> might be considered as the best object for silicon-isotope separation by IR MPD. The molecule contains two Si atoms and the rear isotopes are contained mostly in ‘isotopically mixed’ molecules such as F<sub>3</sub><sup>28</sup>Si-<sup>29</sup>SiF<sub>3</sub> and F<sub>3</sub><sup>28</sup>Si-<sup>30</sup>SiF<sub>3</sub>. This fact limits the isotopic effect since during the dissociation of such ‘isotopically mixed’ molecules, the <sup>28</sup>Si isotope and the rear one, (<sup>29</sup>Si or <sup>30</sup>Si), would pass into products equally. Let us note that in the experiments reported by Kamioka et al. [5, 6] this limit for the <sup>30</sup>Si-isotope enrichment was reached. Besides, we could expect that the isotopic shift of the molecular vibrational frequencies in the ‘isotopically mixed’ molecules would be less than that in the ‘isotopically pure’ molecules.

The above arguments set the problem of searching for molecules containing only one silicon atom and that are at least as effective for isotope-selective IR MPD as Si<sub>2</sub>F<sub>6</sub>. To solve this problem, the systematic quantitative experimental investigation of the infrared multiple photon absorption (IR MPA) and IR MPD of molecules with only one silicon atom is necessary.

Previously, in our group IR MPD of SiF<sub>2</sub>H<sub>2</sub>, CH<sub>3</sub>SiF<sub>3</sub> molecules was studied using pulse CO<sub>2</sub>-laser [11, 12] and IR MPD of C<sub>6</sub>H<sub>5</sub>SiF<sub>3</sub> was studied using free electron laser radiation [13].

The present paper describes the experimental investigation of the main features of the IR MPA and IR MPD of the species C<sub>2</sub>H<sub>3</sub>SiF<sub>3</sub> under the action of a pulsed CO<sub>2</sub>-laser.

## 2 Experiment

All experiments were performed in batch cell conditions, at room-temperature. Samples of neat vinyltrifluorosilane with natural abundance of silicon isotopes were irradiated. In some experiments Br<sub>2</sub> was added to the sample as a radical scavenger. The reaction cell was a Pyrex-glass cylinder with NaCl windows. The cell length was 42 cm; the cell diameter was 3 cm. The cell content was analyzed by a MH-1303 mass spectrometer. The cell was continually con-

✉ Fax: +7 383 3307350, E-mail: gorelik@ns.kinetics.nsc.ru

nected to the ion source of the mass-spectrometer through a glass pinhole of about 20  $\mu\text{m}$  diameter. As a source of IR radiation a homemade tunable pulse TEA CO<sub>2</sub>-laser was used. The maximum pulse energy of the laser was about 5 J. The laser beam was collimated in front of the input window of the cell by an orifice of 1 cm diameter. The energy of the laser radiation pulse was varied by changing the discharge energy and pressure in the laser cavity. To change the pulse energy significantly a set of parallel-sided CaF<sub>2</sub> plates was used. The average energy of the laser radiation was measured in front of the cell and after the cell with an optical power meter. The uniform laser beam was used in almost all experiments. In some experiments on Si isotope-selective IR MPD the laser beam was focused to the center of the reaction cell by a NaCl lens with a focal length of 25 cm.

The parent C<sub>2</sub>H<sub>3</sub>SiF<sub>3</sub><sup>+</sup> ion signals from the mass-spectrometer were measured before and after the irradiation to obtain the Si isotope enrichment.

IR spectra were measured by a fourier transform infrared (FTIR) spectrometer (Bruker Vector 22) with spectral resolution of 1 cm<sup>-1</sup>.

Vinyltrifluorosilane was synthesized by the reaction of vinyltrichlorosilane with antimony trifluoride and consequently purified using a homemade low-temperature rectification column. Vinyltrichlorosilane was received from the A.E. Favorsky Irkutsk Institute of Chemistry SB RAS.

### 3 Computational details

Geometry calculations of the reactants, products and intermediates were performed with the GAUSSIAN98 suit of programs [14]. Those were fully optimized and the fundamental frequencies were calculated using the density functional theory at the hybrid B3LYP level [15, 16] with the 6-31G(p,d) basis set and the unrestricted formalism for the case of radicals. Geometries of transition states (TS) were found using the QST2 procedure [17] and then optimized. The TS geometries were confirmed by frequency calculations of the same level of theory, presenting one imaginary frequency corresponding to the transition vectors pointing in the direction of the reaction coordinate. Local minima structures (reactant and products) were as well confirmed through frequency calculations, which present all frequencies to be necessarily real at local minima.

## 4 Results and discussion

### 4.1 Infrared spectrum

FTIR spectrum of vinyltrifluorosilane in the spectral region of CO<sub>2</sub>-laser radiation is shown in Fig. 1.

The absorption cross-section has been calculated from the measured absorbance, the reaction cell length and the gas pressure. Most of the experiments reported here have been performed when the laser radiation was tuned to the 10P(12) spectral line. This line is indicated in the figure by a vertical arrow. As one can see from Fig. 1 vinyltrifluorosilane has two intensive absorption bands in the 10  $\mu\text{m}$  spectral region with maxima at 892 cm<sup>-1</sup> and at 972 cm<sup>-1</sup>. Following the assignment of Durig et al. [18], the former corresponds to the symmetric stretching vibrational mode ( $\nu_9$ ) of the SiF<sub>3</sub> group,

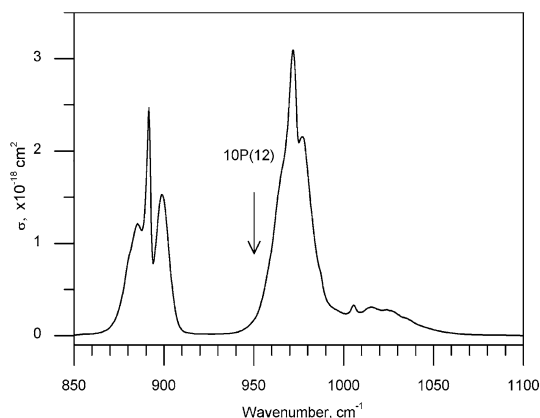


**FIGURE 1** Linear absorption spectrum of vinyltrifluorosilane in spectral region of Si-F stretching vibrations taken at 1 cm<sup>-1</sup> spectral resolution. Vertical line indicates the position of 10P(12) CO<sub>2</sub>-laser line, at which the most part of the experiments have been performed

Experiment, cm <sup>-1</sup> this work	Experiment, cm <sup>-1</sup> [18]	Calculation, cm <sup>-1</sup>			Assignment
		<sup>28</sup> Si	<sup>29</sup> Si	<sup>30</sup> Si	
892	890	894.2	887.7	881.7	$\nu_9$ symmetric
972	970	987.4	980.6	973.8	$\nu_8$ antisymmetric $a'$
972	970	993.0	984.5	976.4	$\nu_{16}$ antisymmetric $a''$

**TABLE 1** Vibrational frequencies of vinyltrifluorosilane in the spectral region of CO<sub>2</sub>-laser. Column 1: experimental results of present work; column 2: experimental results of Durig et al. [18]; column 3–5: calculations for different isotopomers

while the latter corresponds to two antisymmetric vibrations of the SiF<sub>3</sub> group of  $a'$  ( $\nu_8$ ) and  $a''$  species ( $\nu_{16}$ ). DFT calculations of the frequencies of vinyltrifluorosilane have been performed to verify this assignment. The results are presented in Table 1.

The first column of the table presents the values of these frequencies, experimentally obtained here. The second column presents experimental results of Durig et al. [18]. The calculated frequencies are presented in column 3 of the table.

One can see from the table that the agreement between the calculations and the experiment is within 2%. Note, that according to the calculation, the antisymmetric vibrations of  $a'$  and  $a''$  species have slightly different frequencies.

To estimate the isotopic shifts in the IR spectrum the vibrational frequencies of minor Si isotopomers of vinyltrifluorosilane have been calculated in this spectral region. The results are shown in the last two columns of Table 1.

For the stretch vibrations of the SiF<sub>3</sub> group of the vinyltrifluorosilane molecules the calculated isotopic shift for the Si isotopically substituted molecules was found to be about 7–8 cm<sup>-1</sup> for the <sup>29</sup>Si containing molecules and about 15–16 cm<sup>-1</sup> for the <sup>30</sup>Si containing molecules with respect to the <sup>28</sup>Si containing molecules. These values are typical for the Si isotopic shifts in IR spectra of fluorosilanes in the spectral region of Si-F stretch vibrations [3, 13, 19, 20].

### 4.2 Infrared multiphoton absorption and dissociation

Figure 2 presents the laser fluence dependence of  $\langle n \rangle$  – the average number of absorbed photons per molecule, measured at 10P(12) CO<sub>2</sub>-laser line.

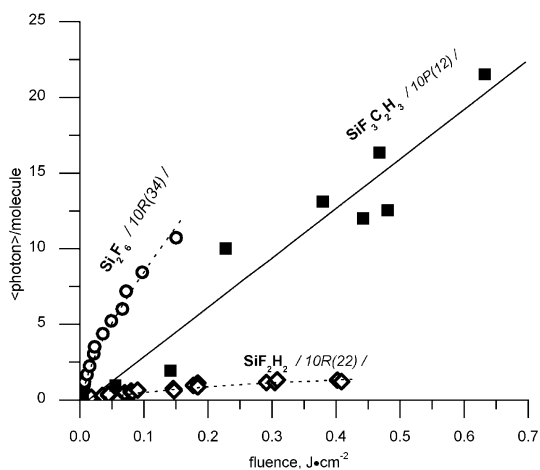


**FIGURE 2** CO<sub>2</sub>-laser radiation energy fluence dependence of IR MPA of vinyltrifluorosilane at 10P(12) laser line (951.19 cm<sup>-1</sup>). Initial sample pressure – about 0.5 Torr. Same dependences for SiF<sub>2</sub>H<sub>2</sub>, taken from [11], and for Si<sub>2</sub>F<sub>6</sub>, taken from [21], are presented as well

This is an important characteristic of the molecule, undergoing the IR MPD, which shows, how effectively the molecule interacts with the laser radiation.

For comparison, the same data for Si<sub>2</sub>F<sub>6</sub> molecules [21] and SiF<sub>2</sub>H<sub>2</sub> molecules [11] are shown. One can see that the absorption of SiF<sub>2</sub>H<sub>2</sub> is strongly saturated even at low radiation fluences. Such behavior is typical for small polyatomic molecules and could be explained by the “rotational bottleneck” effect [22]. In contrast, for vinyltrifluorosilane, as well as for hexafluorodisilane, the dependence is close to linear and no saturation occurs in a wide range of fluences.

Figure 3 presents the laser fluence dependence of IR MPD probability  $\beta$ , an average probability of single molecule to dissociate during the single laser pulse, for vinyltrifluorosilane molecules. It was measured at 10P(12) CO<sub>2</sub>-laser line. For comparison, the same data for Si<sub>2</sub>F<sub>6</sub> molecules [21] and SiF<sub>2</sub>H<sub>2</sub> molecules [11] are shown.

The MPD probability  $\beta$  for vinyltrifluorosilane molecules becomes measurable at fluences higher, than 0.2 J/cm<sup>2</sup> and

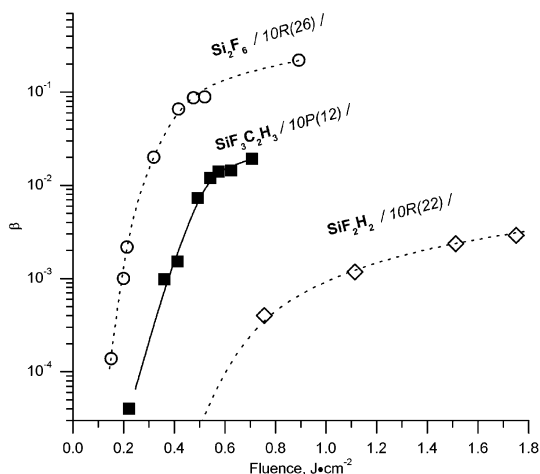


**FIGURE 3** CO<sub>2</sub>-laser radiation energy fluence dependence of IR MPD probability of vinyltrifluorosilane at 10P(12) laser line. Initial pressure – about 0.5 Torr. Same dependences for SiF<sub>2</sub>H<sub>2</sub> and for Si<sub>2</sub>F<sub>6</sub>, taken from literature data [11, 21] are presented as well

reaches values about several percent at the laser fluence of about 0.6 J/cm<sup>2</sup>. Vinyltrifluorosilane dissociates more effectively, than difluorosilane due to the latter possess the rotational bottleneck. At the same time vinyltrifluorosilane dissociates less effectively, than hexafluorodisilane apparently due to the dissociation energy of the latter is essentially low – about 45 kcal/mol [23].

### 4.3 Product analysis

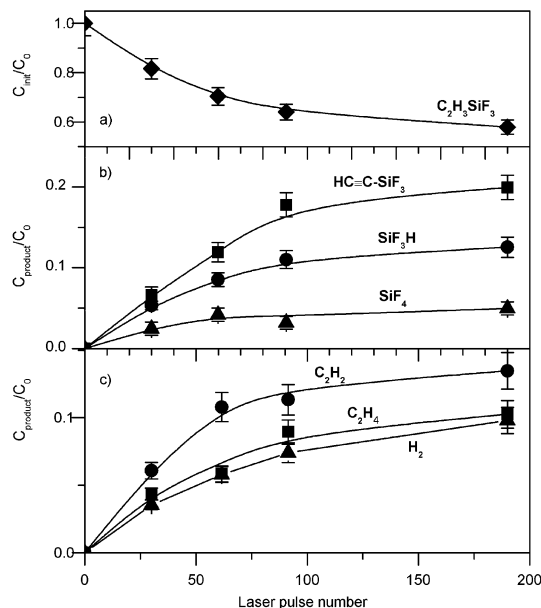
**4.3.1 Experimental results.** Figure 4 shows the evolution of the reaction mixture composition during the irradiation.

Figure 4a shows the reduction of irradiated vinyltrifluorosilane with the laser pulse number, while Fig. 4b shows Si-containing components of the reaction mixture, which concentrations were growing up with increasing the laser pulse number. Other growing up components of the mixture are shown in Fig. 4c.

One can see from Fig. 4 that the main gaseous products of vinyltrifluorosilane multiphoton dissociation were found to be: Si containing SiF<sub>3</sub>H, SiF<sub>3</sub>C<sub>2</sub>H, SiF<sub>4</sub>, hydrocarbons C<sub>2</sub>H<sub>4</sub> and C<sub>2</sub>H<sub>2</sub> and molecular hydrogen H<sub>2</sub>.

In order to obtain extra information about the dissociation channels, additional experiments have been performed in which Br<sub>2</sub> was added to the sample gas as a radical scavenger. The results are represented in Fig. 5.

Figure 5a shows, that the SiF<sub>3</sub>C<sub>2</sub>H<sub>3</sub> IR MPD probability does not change in a range of 0–0.6 Torr of Br<sub>2</sub> concentration. At the same time, SiF<sub>4</sub> and C<sub>2</sub>H<sub>4</sub> product concentrations decrease with increasing Br<sub>2</sub> concentration and vanish completely at about 100 mTorr of Br<sub>2</sub>, while the SiF<sub>3</sub>H concentra-



**FIGURE 4** Evolution of the reaction mixture components during the irradiation process: (a) laser pulse number dependence of vinyltrifluorosilane concentration  $C_{init}/C_0$ , (b) laser pulse number dependence of concentrations of Si containing end products  $C_{product}/C_0$ , (c) laser pulse number dependence of concentrations of Si non-containing end products  $C_{product}/C_0$ , normalized to initial concentration of vinyltrifluorosilane  $C_0$ . CO<sub>2</sub>-laser line: 10 P(12); laser fluence: about 1 J/cm<sup>2</sup>; initial pressure of vinyltrifluorosilane – about 0.4 Torr

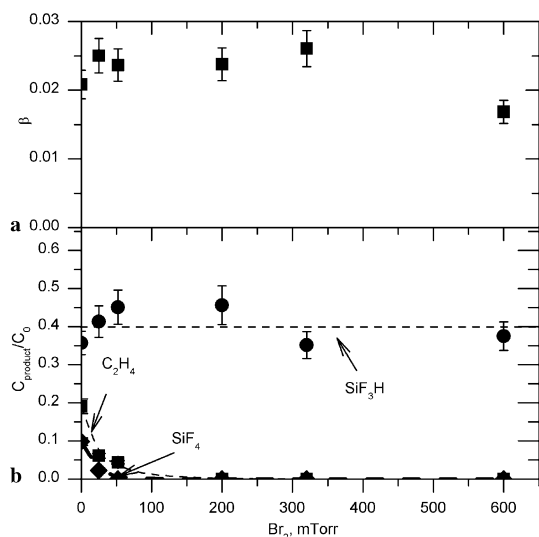
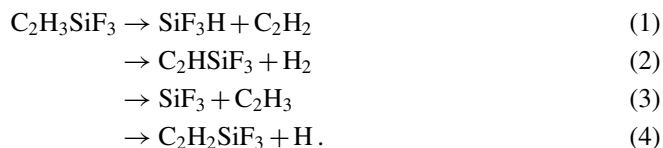


**FIGURE 5** Dependence of the MPD probability  $\beta$ , (a) and relative concentrations of  $\text{SiF}_3\text{H}$ ,  $\text{SiF}_4$ ,  $\text{C}_2\text{H}_4$  end products  $C_{\text{product}}$ , normalized to initial  $\text{C}_2\text{H}_3\text{SiF}_3$  concentration  $C_0$ , (b) on the  $\text{Br}_2$  radical scavenger pressure. The  $\text{CO}_2$ -laser line was 10P(12); laser fluence was about  $1.2 \text{ J/cm}^2$ ; initial pressure of vinyltrifluorosilane was about 0.4 Torr

tion reveals no dependence on  $\text{Br}_2$  pressure (Fig. 5b). Besides,  $\text{SiF}_3\text{Br}$  and  $\text{HBr}$  products were found to appear as MPD products and increase in concentration when  $\text{Br}_2$  concentration increased.

**4.3.2 Calculation results.** To elucidate the primary dissociation pathways, which could lead to the observed end products, quantum chemical calculations of the parameters of different vinyltrifluorosilane decomposition pathways have been performed. According to the calculation, the energetically lowest pathways were found to be:



In pathways (1), (2) molecular products are formed, while pathways (3), (4) lead to the formation of radical products. A schematic presentation of the pathways (1)–(4) is shown in Fig. 6 and the relative energies of the reactant, transition states (TS) and products are shown in Table 2.

Optimized geometric parameters of the reagent, transition states, intermediate and some products are shown in Table 3. Calculated frequencies as well as rotational constants of corresponding species are shown in Table 4.

Pathway (1) leads to the formation of  $\text{SiF}_3\text{H}$  and  $\text{C}_2\text{H}_2$  molecular products. It corresponds to the shift of an H-atom from C-atom in beta position to Si-atom and simultaneous Si–C bond cleavage. TS1 is a transition state for this pathway. Pathway (2) leads to the formation of  $\text{C}_2\text{HSiF}_3$  and  $\text{H}_2$  molecular products. According to the calculation, it consists of two stages. The first stage is a formation of  $\text{CH}_3\text{–C–SiF}_3$  singlet carbon. This stage corresponds to the shift of H-atom from alpha C-atom to beta C-atom. It goes through a transition

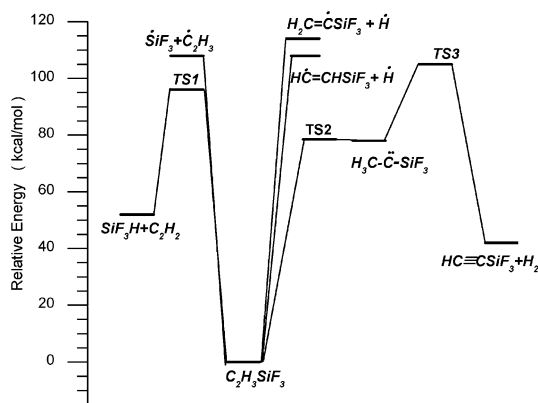


**FIGURE 6** Energetics of the vinyltrifluorosilane decomposition pathways, calculated with B3LYP/6-31G(p,d)

species	$E_{\text{rel}}$ , kcal/mol
$\text{C}_2\text{H}_3\text{SiF}_3$	0
TS1	96.3
$\text{C}_2\text{H}_2 + \text{SiF}_3\text{H}$	52.5
TS2	78.4
$\text{H}_3\text{C–C–SiF}_3$	77.9
TS3	105.4
$\text{HC}\equiv\text{C–SiF}_3 + \text{H}_2$	46.0
$\text{C}_2\text{H}_3 + \text{SiF}_3$	108.2
$\text{HC=CHSiF}_3 + \text{H}$	108.9
$\text{H}_2\text{C=CSiF}_3 + \text{H}$	114.5

**TABLE 2** Calculated relative energies of transition states (TS) and products of possible channels of vinyltrifluorosilane unimolecular decomposition

state TS2. Second stage is the molecular hydrogen detachment from beta C-atom and following formation of CC triple bond. It goes through a transition state TS3.

Pathway (3) corresponds to the Si–C bond cleavage. Pathway (4) corresponds the C–H bond cleavage, where C-atom could be both in alpha and beta position with respect to the Si atom. We assumed that no activation barriers exist for pathways (3), (4).

**4.3.3 Discussion.** Figure 7 presents the same quantities as Fig. 4b – relative concentrations of the main Si containing products of the dissociation versus the relative concentration of the dissociated vinyltrifluorosilane  $\Delta C_{\text{init}}/C_0 = (C_0 - C_{\text{init}})/C_0$  (Fig. 4a). Figure 8 presents the dependences of the C-containing products and molecular hydrogen on the dissociated vinyltrifluorosilane  $\Delta C_{\text{init}}$ . All the concentrations were normalized to the initial concentration of vinyltrifluorosilane  $C_0$ . All the measured dependences, shown in Figs. 7 and 8, were approximated by linear functions passing through (0,0) point.

One can see from Figs. 7 and 8 that the slopes of the linear approximation for  $\text{SiF}_3\text{H}$  and  $\text{C}_2\text{H}_2$  formation dependences are almost equal. Therefore, we can assume that they are formed in the same reactions. Such reactions could be the primary dissociation channel (1) and probably secondary reactions, such as the reaction of  $\text{SiF}_3$  with  $\text{C}_2\text{H}_3$ . In experiments with  $\text{Br}_2$ ,  $\text{SiF}_3\text{H}$  concentration does not depend on the concentration of  $\text{Br}_2$  (Fig. 5b). This fact indicates that  $\text{SiF}_3\text{H}$  and, hence,  $\text{C}_2\text{H}_2$  are formed in the primary dissociation channel (1).

elements	C <sub>2</sub> H <sub>3</sub> SiF <sub>3</sub>			CH <sub>3</sub> -C-SiF <sub>3</sub> (carben)			HC≡C-SiF <sub>3</sub>		
	x-coord	y-coord	z-coord	x-coord	y-coord	z-coord	x-coord	y-coord	z-coord
Si	0.369463	0	0	-0.03603	0.000069	0.391181	0.000108	-4.1E-05	0.328056
C	-1.25883	0	0.844479	-0.82052	0.022262	-1.29594	0.000262	-0.00024	-1.46783
C	-2.39752	0	0.140502	0.033534	-0.05284	-2.454	0.000169	-4.4E-05	-2.6801
F	0.154393	0	-1.5813	-0.3441	1.385952	1.116462	-0.62149	1.349478	0.890135
F	1.247229	1.278919	0.373196	-0.7074	-1.19382	1.205503	1.479377	-0.13664	0.890887
F	1.247229	-1.27892	0.373196	1.549808	-0.21307	0.486335	-0.85834	-1.21261	0.89039
H	-2.39502	0	-0.9463	1.058639	-0.45167	-2.41771	-2.7E-05	0.00022	-3.7479
H	-3.37443	0	0.618063	0.137184	1.07459	-2.41871	-	-	-
H	-1.30456	0	1.932546	-0.45425	-0.25199	-3.41521	-	-	-

elements	TS1			TS2			TS3		
	x-coord	y-coord	z-coord	x-coord	y-coord	z-coord	x-coord	y-coord	z-coord
Si	-0.00002	0.082519	-0.26366	-0.03643	0.008763	0.378622	-0.05925	0.00001	0.384195
C	0.000105	-0.38894	1.770199	-0.7851	0.144387	-1.30711	-0.87898	0.000124	-1.23013
C	0.000036	0.865431	1.844926	0.057279	0.063106	-2.42924	-0.21878	0.000037	-2.37254
F	-1.37814	-0.73372	-0.4116	-0.6149	-1.27829	1.122518	-0.44287	1.294753	1.228683
F	-0.00014	0.787338	-1.72759	-0.4489	1.315074	1.192469	-0.44389	-1.29422	1.229022
F	1.378251	-0.73342	-0.41182	1.560898	-0.10744	0.471472	1.544941	-0.00061	0.256341
H	0.00008	1.512601	0.342242	-0.38999	-1.00605	-2.11161	-0.50198	0.000222	-3.41911
H	-0.00076	1.8672	2.238014	-0.36483	0.196199	-3.43235	0.997333	0.459507	-2.38492
H	0.000436	-1.27581	2.379179	1.157907	0.078143	-2.41683	0.997046	-0.46014	-2.38509

**TABLE 3** The B3LYP/6-31G(p,d) Optimized Geometric Parameters for the Species C<sub>2</sub>H<sub>3</sub>SiF<sub>3</sub>, SiF<sub>3</sub>CCH, CH<sub>3</sub>CSiF<sub>3</sub> and Transition States TS1, TS2, TS3 (see details in the text). Cartesian coordinates of atoms are shown in Angstroms

species	frequency, cm <sup>-1</sup>	rot const, cm <sup>-1</sup>
C <sub>2</sub> H <sub>3</sub> SiF <sub>3</sub>	79.6, 170.5, 197.6, 280.9, 323.3, 352.9, 430.4, 557.8, 684.0, 894.4, 988.0, 993.0, 1021.5, 1038.6, 1046.4, 1300.4, 1457.0, 1678.0, 3148.1, 3164.2, 3235.6	0.073, 0.071, 0.131
H <sub>3</sub> C-C-SiF <sub>3</sub>	58.4, 113.8, 224.5, 257.8, 296.1, 342.7, 384.2, 410.2, 478.8, 636.4, 879.7, 976.1, 1003.5, 1103.6, 1230.1, 1286.7, 1321.9, 1544.3, 2781.9, 2999.5, 3080.1	0.070, 0.070, 0.127
HC≡CSiF <sub>3</sub>	136.9, 137.6, 282.3, 282.4, 357.1, 399.2, 399.4, 648.8, 710.6, 710.6, 893.7, 1015.1, 1015.4, 2185.7, 3471.3	0.071, 0.071, 0.134
TS1	726.5i, 166.2, 188.8, 193.9, 344.1, 354.9, 393.9, 507.8, 558.0, 610.4, 702.4, 832.0, 841.4, 862.6, 923.7, 997.9, 1265.9, 1789.6, 1999.9, 3306.2, 3364.8	0.082, 0.075, 0.137
TS2	480.3i, 65.2, 124.4, 241.0, 264.8, 304.2, 354.2, 410.9, 576.3, 653.9, 884.5, 974.0, 1005.5, 1062.0, 1134.8, 1268.2, 1392.6, 1564.0, 2389.0, 2995.3, 3079.5	0.071, 0.071, 0.128
TS3	1488.1i, 84.6, 110.0, 242.1, 264.6, 308.1, 358.8, 410.1, 498.1, 635.2, 681.5, 887.0, 934.2, 974.9, 1006.0, 1015.4, 1444.5, 1559.4, 1704.8, 2620.1, 3219.7	0.072, 0.072, 0.131

**TABLE 4** The B3LYP/6-31G(p,d) frequencies and rotational constants of the species C<sub>2</sub>H<sub>3</sub>SiF<sub>3</sub>, SiF<sub>3</sub>C≡CH, CH<sub>3</sub>-C-SiF<sub>3</sub> and Transition Sates TS1, TS2, TS3

In experiments with Br<sub>2</sub> fast drop of SiF<sub>4</sub> and C<sub>2</sub>H<sub>4</sub> concentrations (Fig. 5b), when Br<sub>2</sub> concentration increases, indicates that these products are formed in secondary reactions. Br<sub>2</sub> is a good scavenger for C<sub>2</sub>H<sub>3</sub> [24] and SiF<sub>3</sub> [12] radicals. Besides, in these experiments SiF<sub>3</sub>Br and C<sub>2</sub>H<sub>3</sub>Br end products were found to appear and increase in concentrations with Br<sub>2</sub>. So, we can assume that channel (3) takes place in our experiments, and that SiF<sub>4</sub> appears in reaction of SiF<sub>3</sub> radical disproportionation:



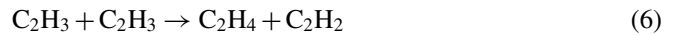
It is well known, that SiF<sub>2</sub> is a very low active radical [25–29]. In our experiments most probably it reaches the walls of the reaction cell, where it forms non-volatile high-molecular compounds [5, 6].

Time, which is necessary for a radical to diffuse to the wall of the reaction cell, can be estimated using the formula [30]:

$$\tau_{\text{diff}} = (0.173R)^2/D,$$

where  $D$  is a diffusion coefficient,  $R$  is a radius of the reaction cell. In our experiments  $R = 1.5$  cm,  $D$  is about 100 cm<sup>2</sup>/s at 0.5 Torr pressure, thus  $\tau_{\text{diff}} \approx 4 \times 10^{-3}$  s.

Since C<sub>2</sub>H<sub>2</sub> molecules are formed only in primary dissociation channel (1), they could not be formed in reactions of C<sub>2</sub>H<sub>3</sub> radicals, such as



According to the literature data reactions (6) and (7) are very fast:  $k_6 = 3.5 \times 10^{-11}$  cm<sup>3</sup>/s,  $k_7 = 2 \times 10^{-11}$  cm<sup>3</sup>/s [31, 32]. If they took place in our experiments, the time of consumption of C<sub>2</sub>H<sub>3</sub> radicals in reactions (6) and (7) under our experimental conditions would be about  $3 \times 10^{-4}$  s and  $5 \times 10^{-4}$  s correspondingly, which is about an order of magnitude shorter than the time of diffusion  $\tau_{\text{diff}}$ . Thus, C<sub>2</sub>H<sub>3</sub> radicals should be consumed in gaseous phase, in reactions, faster than reaction (6), (7). Such reactions could be, for ex-

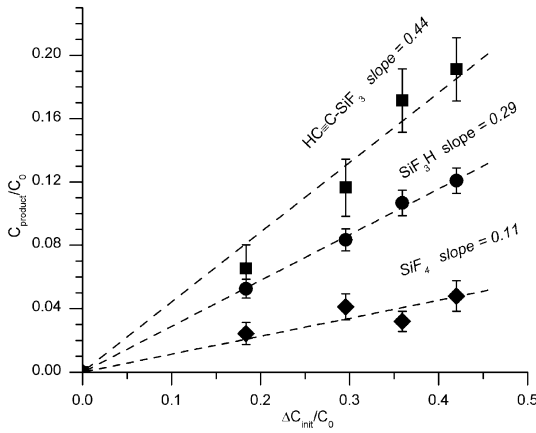


**FIGURE 7** Dependence of the relative concentrations of Si-containing end products on the fraction of dissociated vinyltrifluorosilane. The CO<sub>2</sub>-laser line was 10P(12); laser fluence was about 1.2 J cm<sup>-2</sup>; initial pressure of vinyltrifluorosilane was about 0.4 Torr

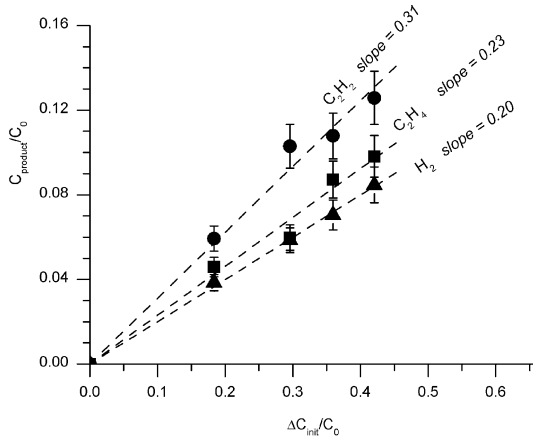
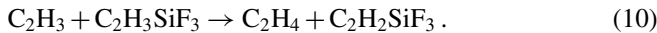
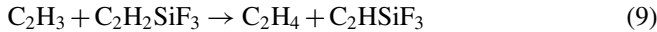


**FIGURE 8** Dependence of the relative concentrations of Si non-containing end products on the fraction of dissociated vinyltrifluorosilane. The CO<sub>2</sub>-laser line was 10P(12); laser fluence was about 1.2 J cm<sup>-2</sup>; initial pressure of vinyltrifluorosilane was about 0.4 Torr

ample:



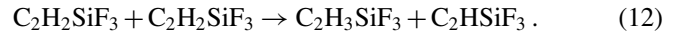
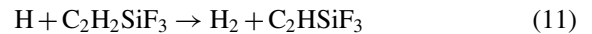
The bimolecular rate constant of reaction (8) at room temperature was measured by Fahr et al. [33] and was found to be very high:  $2.01 \times 10^{-10}$  cm<sup>3</sup>/s. Monks et al. [34] have measured this rate constant at 1 Torr and received about  $3 \times 10^{-11}$  cm<sup>3</sup>/s. They also have estimated high pressure limit  $k_\infty = 1.7 \times 10^{-10}$  cm<sup>3</sup>/s and low pressure limit  $k_0 = 1.4 \times 10^{-27}$  cm<sup>6</sup>/s for the rate constant of reaction (8) using quantum RRR analysis of their experimental data and the experimental data of [33]. Using their data, we estimated the rate constant for reaction (8) as about  $5 \times 10^{-11}$  cm<sup>3</sup>/s for the pressure range of our experiments. In experiments, described in [33, 34], He was used as a buffer gas. In our experiments the buffer gas was polyatomic vinyltrifluorosilane, which should make the rate constant even higher than the estimated value. Therefore, reaction (8) could be faster, than reactions (6) and (7) and should not be neglected under our

experimental conditions. The reaction (9) is a reaction of two radicals, in which two neutral molecules are formed. Such a reaction should not have an activation barrier, and we can expect reaction (9) to be quite fast. Reaction (10) is a reaction of C<sub>2</sub>H<sub>3</sub> radical with the parent molecule. According to quantum chemical calculation  $\Delta H_0$  for this reaction was found to be close to 0. Hence, according to the Polanyi–Semenov rule [35], the activation barrier for this reaction could be estimated as about 10 kcal/mol, and the higher limit for the rate constant of this reaction could be estimated as about  $k_{10} \leq 10^{-17}$  cm<sup>3</sup>/s, which makes this reaction too slow to compete with reaction (6) and (7). However, during the irradiation process most part of the parent molecules become highly vibrationally excited, which could make this reaction much faster; therefore, it can not be neglected.

Thus, we can assume that, one C<sub>2</sub>H<sub>3</sub> radical turns into one C<sub>2</sub>H<sub>4</sub> molecule and all C<sub>2</sub>H<sub>3</sub> are transformed into C<sub>2</sub>H<sub>4</sub>. The slope of the dependence of C<sub>2</sub>H<sub>4</sub> formation in Fig. 7 is about 0.25, which is about twice higher, than the slope of SiF<sub>4</sub> formation in Fig. 6 (about 0.12). Since two SiF<sub>3</sub> radicals give one SiF<sub>4</sub> molecule via reaction (5), we can assume that all SiF<sub>3</sub> radicals were consumed in this reaction and no other reactions of SiF<sub>3</sub> radicals occurred.

Thus, we can conclude, that all observed SiF<sub>3</sub>H and C<sub>2</sub>H<sub>2</sub> end products could be formed only in primary dissociation pathway (1); all observed SiF<sub>4</sub> and C<sub>2</sub>H<sub>4</sub> end products could be formed only in secondary reactions of C<sub>2</sub>H<sub>3</sub> and SiF<sub>3</sub> radicals, appearing in primary dissociation channel (3).

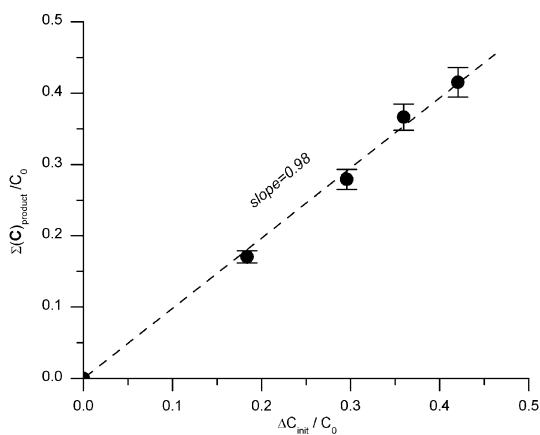
If HC<sub>2</sub>SiF<sub>3</sub> and H<sub>2</sub> end products were formed only in channel (2), the slopes of the corresponding lines in Figs. 7 and 8 would be equal. But the slope of HC<sub>2</sub>SiF<sub>3</sub> formation is about twice as high as that of H<sub>2</sub> formation. Thus, H<sub>2</sub> and HC<sub>2</sub>SiF<sub>3</sub> are formed in different reactions, which should be secondary reactions of the radicals, formed in channel (4). For example, in addition to channel (2), HC<sub>2</sub>SiF<sub>3</sub> molecules could be formed in secondary reactions of C<sub>2</sub>H<sub>2</sub>SiF<sub>3</sub> radical, such as reaction (9) and reactions



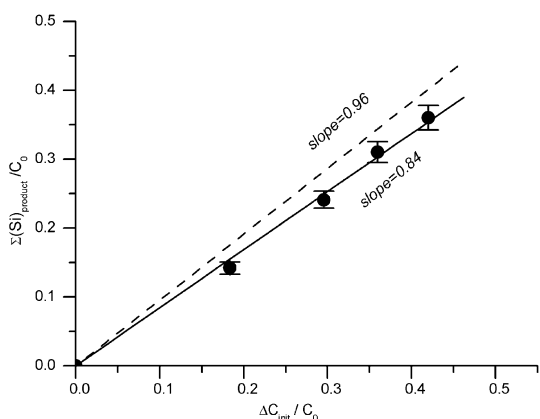
Apart from the primary dissociation channel (2), H<sub>2</sub> could be formed in secondary reactions, such as reaction (11) and the recombination reaction  $\text{H} + \text{H} \rightarrow \text{H}_2$ .

Figure 9 presents the dependence of the relative carbon elemental contents in products on that in the dissociated vinyltrifluorosilane. One can see that the slope of this dependence is close to 1. It means that no C-containing non-volatile products are formed, and in particular, that all products of reactions of C containing radicals are gaseous.

Figure 10 shows the dependence of relative silicon elemental contents in products on that in the dissociated vinyltrifluorosilane. It could be approximated by a line with a slope of about 0.85. To take into account the SiF<sub>2</sub> fragment, we should double the concentration of SiF<sub>4</sub>, when estimating the Si elemental contents in products, since SiF<sub>4</sub> and SiF<sub>2</sub> should be formed in equal proportion via reaction (5). Consequently, we will obtain the dependence, presented in Fig. 10 by the dashed line. One can see that the slope of this constructed dependence is close to 1. Therefore, we can conclude that SiF<sub>2</sub> is



**FIGURE 9** Dependence of relative elemental contents of carbon in products on that in the dissociated vinyltrifluorosilane. All the quantities are normalized per initial vinyltrifluorosilane concentration  $C_0$



**FIGURE 10** Dependence of relative elemental contents of silicon in products on that in the dissociated vinyltrifluorosilane. All the quantities are normalized per initial vinyltrifluorosilane concentration  $C_0$

the only Si-containing product, which forms the non-volatile compounds, and all products of reactions of other Si containing radicals are apparently gaseous. Thus, Figs. 9 and 10 confirm indirectly the arguments set above.

From Figs. 7 and 8 the channel ratio of primary dissociation pathways (1)–(4) under our experimental conditions can be estimated. From the above considerations it could be concluded that in our experiments vinyltrifluorosilane molecules could be possibly consumed in primary dissociation channels (1)–(4) and in secondary reaction (10) of vinyl radicals with vibrationally excited vinyltrifluorosilane molecules.

One can see, that the fraction of channel (1),  $f_1 \approx 0.3$ , fraction of channel (3),  $f_3 \approx 0.25$ . Since molecular hydrogen could be formed not only in primary channel (2), but also in secondary reactions, we can estimate an upper limit for channel (2) fraction:  $f_2 \leq 0.2$ . Primary channel (4) cannot be separated from reaction (10) from our experimental data. We could conclude only, that their fractions in sum give  $f_4 + f_{10} \approx 1 - (f_1 + f_2 + f_3) \geq 0.25$ .

#### 4.4 Si isotope selective IR MPD of vinyltrifluorosilane

Experiments on Si isotope selective IR MPD were performed with neat vinyltrifluorosilane, at 0.1 Torr pres-

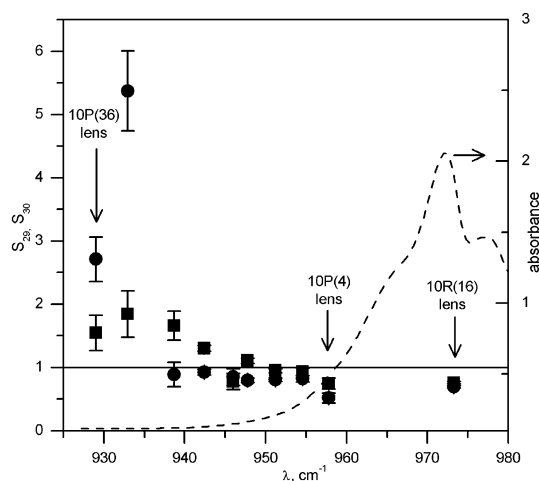


**FIGURE 11** Dependence of isotopic selectivities  $S_{29}$  (■),  $S_{30}$  (●) (see the text for details) on the laser radiation wavelength. Initial pressure of vinyltrifluorosilane was about 0.1 Torr. All points of the dependence were obtained using uniform laser beam of about  $1 \text{ J/cm}^2$  energy fluence, except for the points indicated by vertical arrows, at which the laser beam was focused. Solid horizontal line corresponds to  $S = 1$ . The dashed line shows the linear absorption spectrum in this region (right y-axis; 2.5 Torr, 18 cm)

sure. Isotope selectivity was determined as a ratio of dissociation probabilities of parent molecules with different isotopes. Thus, isotope selectivity for  $\text{C}_2\text{H}_3^{29,30}\text{SiF}_3$  isotopomers would be  $S_{29,30} = \beta_{29,30}/\beta_{28}$ , where  $\beta_i$  is a dissociation probability of the  $i$ th isotopomer. Figure 11 presents the wavelength dependence of  $S_{29}$  and  $S_{30}$ . Most of the experiments have been performed with unfocused beam. The laser beam was focused into the center of the reaction cell for those laser lines, at which the fluence of unfocused beam was not sufficient to dissociate the molecules. The points, which have been obtained using the focused laser beam, are indicated in the figure with vertical arrows. One can see that each isotopomer could be preferentially dissociated, depending on the wavelength of irradiation. The maximum selectivity that was reached in our experiments, was  $S_{30} \approx 5.5$ ,  $S_{29} \approx 2$ .

## 5 Conclusion

Si isotope selective infrared multiphoton dissociation of vinyltrifluorosilane was experimentally studied. The molecule can absorb many IR photons without saturation. Using quantum chemical calculation, we determined the pathways of the IR MPD of vinyltrifluorosilane and their ratio under the experimental conditions used. As follows from the quantum chemical calculation, the dissociation energy of the vinyltrifluorosilane is close to 100 kcal/mol. For the  $\text{Si}_2\text{F}_6$  molecule it is about 45 kcal/mol. Apparently, this is one of the main reasons, why the isotopic selectivities for the IR MPD of vinyltrifluorosilane were found to be lower than for  $\text{Si}_2\text{F}_6$  [5, 6].

**ACKNOWLEDGEMENTS** Authors are grateful to Professor N.P. Gritsan (Institute of Chemical Kinetics and Combustion) for helpful discussion and to Professor V.I. Rakhlin of the Favorsky Institute of Chemistry for providing vinyltrichlorosilane. This work was supported by the Siberian Branch of the Russian Academy of Science (Grant No. 174/03).

## REFERENCES

- 1 W.S. Capinski, H.J. Maris, E. Bauser, E. Silier, M. Asen-Palmer, T. Ruf, M. Cardona, E. Gmelin, *Appl. Phys. Lett.* **71**, 2109 (1997)
- 2 K. Takyu, K.M. Itoh, K. Oka, N. Saito, V.I. Ozhogin, *Jpn. J. Appl. Phys.* **38**, 1493 (1999)
- 3 J.L. Lyman, S.D. Rockwood, *J. Appl. Phys.* **47**, 595 (1976)
- 4 N.K. Serdyuk, E.N. Chesnokov, V.N. Panfilov, *React. Kinet. Catal. Lett.* **17**, 19 (1981)
- 5 M. Kamioka, S. Arai, Y. Ishikawa, S. Isomura, N. Takamiya, *Chem. Phys. Lett.* **119**, 357 (1985)
- 6 M. Kamioka, Y. Ishikawa, H. Kaetsu, S. Isomura, S. Arai, *J. Phys. Chem.* **90**, 5727 (1986)
- 7 H. Suzuki, H. Araki, T. Noda, *J. Jpn. Inst. Met.* **61**, 145 (1997)
- 8 J.L. Lyman, B.E. Newman, T. Noda, H. Suzuki, *J. Phys. Chem. A* **103**, 4227 (1999)
- 9 M. Kamioka, Y. Ishikawa, S. Arai, S. Isomura, N. Takamiya, *Laser Sci. Prog. Rep. IPCR.* **7**, 57 (1985)
- 10 D.R. Lide (Ed.), *CRC Handbook of Chemistry and Physics* (CRC Press, 1998), 79th edn., p. 11–43
- 11 S.R. Gorelik, E.N. Chesnokov, L.V. Kuibida, R.R. Akberdin, A.K. Petrov, *Appl. Phys. B* **78**, 119 (2004)
- 12 P.V. Koshliakov, E.N. Chesnokov, S.R. Gorelik, V.G. Kiselev, A.K. Petrov, *Khim. Fiz.* **25**, 12 (2006)
- 13 A.V. Chernyshev, K. Nomaru, A.K. Petrov, E.N. Chesnokov, S.R. Gorelik, L.V. Kuibida, R.R. Akberdin, H. Kuroda, *J. Phys. Chem. A* **107**, 9362 (2003)
- 14 M.J. Frisch, G.W. Trucks, H.B. Schlegel, G.E. Scuseria, M.A. Robb, J.R. Cheeseman, V.G. Zakrzewski, J.A. Montgomery Jr., R.E. Stratmann, J.C. Burant, S. Dapprich, J.M. Millam, A.D. Daniels, K.N. Kudin, M.C. Strain, O. Farkas, J. Tomasi, V. Barone, M. Cossi, R. Cammi, B. Mennucci, C. Pomelli, C. Adamo, S. Clifford, J. Ochterski, G.A. Petersson, P.Y. Ayala, Q. Cui, K. Morokuma, D.K. Malick, A.D. Rabuck, K. Raghavachari, J.B. Foresman, J. Cioslowski, J.V. Ortiz, A.G. Baboul, B.B. Stefanov, G. Liu, A. Liashenko, P. Piskorz, I. Komaromi, R. Gomperts, R.L. Martin, D.J. Fox, T. Keith, M.A. Al-Laham, C.Y. Peng, A. Nanayakkara, C. Gonzalez, M. Challacombe, P.M.W. Gill, B.G. Johnson, W. Chen, M.W. Wong, J.L. Andres, M. Head-Gordon, E.S. Replogle, J.A. Pople, Revision A.6–A.11 Gaussian, Inc., Pittsburgh, PA (1998)
- 15 A.D. Becke, *J. Chem. Phys.* **98**, 5648 (1993)
- 16 C. Lee, W. Yang, R.G. Parr, *Phys. Rev. B* **37**, 785 (1998)
- 17 L.A. Curtiss, K. Raghavachari, G.W. Trucks, J.A. Pople, *J. Chem. Phys.* **94**, 7221 (1991)
- 18 J.R. Durig, K.L. Hellams, *J. Mol. Struct.* **6**, 315 (1970)
- 19 E.N. Chesnokov, S.R. Gorelik, N.P. Gritsan, *Vib. Spectrosc.* **32**, 241 (2003)
- 20 E.N. Chesnokov, P.V. Koshliakov, S.R. Gorelik, *Opt. Spectrosc.* **99**, 910 (2005) (in Russian)
- 21 V. Tosa, S. Isomura, K. Takeuchi, *J. Photochem. Photobiol. A* **91**, 1731 (1995)
- 22 V.S. Letokhov, A.A. Makarov, *JETP* **63**, 2064 (1972)
- 23 S.K. Bains, P.N. Noble, R. Walsh, *J. Chem. Soc. Faraday Trans. 2* **82**, 837 (1986)
- 24 R.S. Timonen, J.A. Seetula, D. Gutman, *J. Phys. Chem.* **97**, 8217 (1993)
- 25 M. Koshi, S. Kato, H. Matsui, *J. Phys. Chem.* **95**, 1223 (1991)
- 26 M.Y. Skok, E.N. Chesnokov, *Khim. Fiz.* **7**, 228 (1988) (in Russian)
- 27 A.C. Station, A. Freedman, J. Wormhoudt, P.P. Gasper, *Chem. Phys. Lett.* **122**, 190 (1985)
- 28 A. Freedman, K.E. McCurdy, J. Wormhoudt, P.P. Gasper, *Chem. Phys. Lett.* **142**, 255 (1987)
- 29 K. Sugawara, F. Ito, T. Nakanaga, H. Takeo, *Chem. Phys. Lett.* **232**, 561 (1995)
- 30 E.T. Denisov, *Kinetics of Homogeneous Chemical Reactions* (Vysshiaia shkola, Moscow, 1978) (in Russian)
- 31 A.H. Laufer, A. Fahr, *Chem. Rev.* **104**, 2813 (2004)
- 32 D.L. Baulch, C.J. Cobos, R.A. Cox, C. Esser, P. Frank, T. Just, J.A. Kerr, M.J. Pilling, J. Troe, R.W. Walker, J. Warnatz, *J. Phys. Chem. Ref. Data* **21**, 411 (1992)
- 33 A. Fahr, A. Laufer, R. Klein, W. Braun, *J. Phys. Chem.* **95**, 3218 (1991)
- 34 P.S. Monks, F.L. Nesbitt, W.A. Payne, M. Scanlon, L.J. Stief, D.E. Shallcross, *J. Phys. Chem.* **99**, 17151 (1995)
- 35 V.N. Kondratiev, E.E. Nikitin, *Kinetics and Mechanisms of Gas Phase Reactions* (Nauka, Moscow, 1974) (in Russian)